OATAO
Open Archive Toulouse Archive Ouverte

Open Archive Toulouse Archive Ouverte (OATAO)

OATAO is an open access repository that collects the work of Toulouse researchers and makes it freely available over the web where possible.

Effects of membrane alterations on bacterial retention

Nathalie Lebleu[a,b], Christine Roques[c], Pierre Aimar[a,b], Christel Causserand[a,b,*]

[a] *Université de Toulouse, INPT, UPS, Laboratoire de Génie Chimique, 118 Route de Narbonne, F-31062 Toulouse, France*
[b] *CNRS, Laboratoire de Génie Chimique, F-31062 Toulouse, France*
[c] *LU 49, Equipe Adhésion Bactérienne et Formation de Biofilms, Université Paul Sabatier, 31062 Toulouse cedex 09, France*

ABSTRACT

The study shows the respective roles of skin and support of an ultrafiltration membrane in the retention mechanisms of bacteria (*Escherichia coli*). For this, pinholes defects of 5–200 μm in diameter were performed through ultrafiltration polymeric membranes and their impact was assessed on bacterial retention in a stirred cell when the transmembrane pressure is set at 0.5 bars. Various techniques have been used to make the defects such as a microhardness tester or femtosecond lasers. As long as the selective skin is not altered through its whole thickness, the membrane keeps a retention efficiency equivalent to the one of an uncompromised membrane. The retention by the macroporous support is also investigated.

In case of membrane with defects of cylindrical geometry, experimental results are compared to calculated data obtained with a pore flow model, and the validity of this model is discussed.

1. Introduction

One of the major advantages of membrane filtration over more conventional processes in water treatment is their efficiency for the retention of microorganisms, which have become of major concern. The membranes act as physical screens, precluding the transfer of bacteria, fungi, algae or protozoan. Ultrafiltration is well-adapted to remove waterborne microorganisms of 1 μm for bacteria and of 5 μm for protozoan such as *Cryptosporidium parvum* from natural waters and thus to meet drinking water regulation [1].

As the infectious dose of some waterborne pathogens could be very low (for instance around 100 cells/mL for *Cryptosporidium parvum*), processes must show a high retention for microorganisms over their life time, and in the full range of operating situations which can be implemented in a plant. The presence of a few defects through a membrane can allow enough microorganisms through to make the permeate inappropriate for further use, according to the relevant regulation.

Such defects can exist *ab initio* in membranes or in systems (gaskets, potting, etc.) but the risk is generally well reduced by severe tests run at the production level and before implementing a system. Among them, the pressure decay test (PDT) which is a gas–liquid diffusion test. The principle is based on a wetted membrane which provides a liquid layer across which diffusive air flow occurs according to the Fick's law. An air flow rate larger than predicted signals the presence of a defect. However, the sensitivity of this test is limited by the minimum detectable excess flow which allows only the detection of defects larger than around 3 μm in diameter [2–4]. As a consequence, this test is not sensitive enough to detect some smaller imperfections, such as abnormally large pores which may be generated during membranes fabrication and are likely to allow unexpected bacterial leakages according to the size of the targeted microorganisms.

The pore size distribution of a UF membrane depends on the manufacturing method. For membranes produced by phase inversion, the pore size distribution has been approximated by a unimodal log-normal law which includes a tail of large pores sizes [5]. However, this distribution is not sufficient to explain the presence of bacteriophages in the permeate [6]. The authors assume that the leakages result from the presence of a few oversized pores as compared to the average pore rating (around 10 nm). Assuming a unique diameter for these defects (100 nm), the discrepancy between the bacteriophages experimental rejection and the calculated one according to the log-normal distribution, they evaluate the ratio defects/normal pores at $1/10^9$. Thus, even limited numbers, large pores are likely to have a significant impact on particles rejection.

This assumption is also used by Kobayashi et al. [7] and Shinde et al. [8] to justify bacterial leakages through asymmetric ultrafiltration membranes. Kobayashi et al. [7] show that when operating conditions used for membrane fabrication generate fingerlike

* Corresponding author at: Université de Toulouse, INPT, UPS, Laboratoire de Génie Chimique, 118 Route de Narbonne, F-31062 Toulouse, Cedex 9, France. Tel.: +33 5 61 55 86 90; fax: +33 5 61 55 61 39.

E-mail address: caussera@chimie.ups-tlse.fr (C. Causserand).

macrovoids, these may reach up the skin layer and therefore allow the microorganisms to pass through.

In addition, this unexpected transfer could be enhanced by the bacterial deformation which allows their transfer through pores smaller than their dimension [9–11]. Sucheka et al. [10] suggest that the essential condition of this process is a change of the bacteria volume, which should be accompanied by a partial outflow of the intracellular material through the cell wall.

Over a membrane and module lifetime, the membrane porous structure may be altered by repeated chemical and mechanical cleaning procedures. Those alterations result in changes in the membrane mechanical properties which, in the worst case, can lead in hollow fiber systems to the breakage of a fiber [12]. For instance, by gathering data from the literature and information from membrane manufacturers or water treatment plants, Gijsbertsen-Abrahamse et al. [13] show that the fiber failure rate corresponds to up to one broken fiber per module per year. These defects are quite easily detected by on-line turbidity monitoring or other particle counting systems, as the permeate pollution inferred by the breakage is concentrated enough to be detected by standard measurement devices.

However, modules autopsy reveals that some fractures do not consist in total cracking of the fiber but in small breaches more difficult to detect [13]. These smaller defects can occur either by scratches or by cracks appearing at the membrane surface. The scratches can be produced by inorganic particles circulated through the system and produced by detachment of small bits of material (scaling layers, plastics or else) due to mechanical stresses accompanying backwashing procedures. The cracks may appear due to membrane material ageing, under the strain produced by the combination of the chemical and mechanical treatments applied to fight against fouling.

In this context, Gitis et al. [14,15] studied the relationship between the integrity loss due to accelerated chemical ageing of ultrafiltration membranes and their efficiency in terms of MS2 bacteriophages rejection. They show that the membrane structure alteration can be splitted in a two-stage mechanism. The first stage involves the formation of holes with an average diameter of 20–30 nm (i.e. two or three times larger than the initial mean pore diameter). The second stage consists in the rapid growth of these holes leading to disintegration of the skin layer. The loss in membrane rejection efficiency is detected as soon as the ageing mechanism is initiated and the gradual evolution of the membrane structure is consistent with the evolution of the bacteriophages transfer to the permeate compartment.

Whatever the origin of these defects in the porous membrane structure, they are likely to allow microorganisms through. Membrane characterization is then an issue, which justifies a lot of efforts in research and production control as most of the available characterization methods are not sensitive enough to reveal such potential.

Causserand et al. [16] show that the water permeability and the molecular weight cut-off (obtained by dextrans rejection), are not modified by the presence of a 50 µm diameter defect generated by a sharp tip upon a 13.4 cm^2 ultrafiltration membrane (equivalent to *ca* 750 defects/m^2). Rejection of macromolecules such as polyethylene glycols or dextrans allow to estimate a pore size distribution but not to detect few abnormally large pores likely to allow microorganisms through [6,7]. This latter study shows that analytical methods used in standard protocols for the determination of the molecular sieving curves are not accurate enough to predict the retention of microorganisms.

Methods based on the displacement of an air/liquid interface such as bubble point measurements and pressure decay tests are more sensitive to the presence of defects. Adams and Côté [3] propose a correlation of the log reduction value obtained experimentally after the filtration of a *Bacillus subtilis* suspension to the one predicted by air-based test results. Their results were obtained by experimental trials on hollow fibers modules including deliberately compromised fibers (breakage or pinhole) and by describing the flow through the defect by Hagen-Poiseuille's law. Thus, they show that, depending on the tested membrane, the log reduction value obtained during the filtration of *Bacillus subtilis* is either superior or similar to that estimated from the integrity test data which can therefore be used, in those conditions, to predict microorganism's removal. However, as the diameter of the defect is not specified, it could be much larger than the detection limit of the integrity test (around 3 µm) which casts doubt on the validity of this correlation.

Giglia and Krishnan [4] develop an integrity test more sensitive in terms of diameter to defects than conventional gas–liquid diffusion tests. This test is based on gas mixture of two components with different permeabilities and on the measurements of the downstream gas composition instead of the downstream flow rate. The authors demonstrate that, unlike classical gas–liquid diffusion methods, this one is able to detect a single defect of 2 µm (performed by laser drilling on a membrane of 127 cm^2 effective filtration area). Moreover, in the range from 2 to 10 µm diameters, the loss in bacteriophages log reduction value due to a defect of controlled size compared to a defect-free membrane can be predicted from calculation based on the binary gas value and Hagen-Poiseuille's laws for compressible and non-compressible fluids.

From this literature survey it appears that the structure, the frequency and the location of defects in UF membranes is rather ill documented, and the detection of such defects is therefore pretty difficult, especially for small number of small defects.

With the objective of understanding the possible role of such rare defects on the contamination of ultrafiltration permeates, we decided to make pinholes in some membranes which were fully rejective towards the selected microorganism when uncompromised, and to measure the bacterial leakage through such corrupted membranes. Influence of the defect characteristics (number, size, depth of penetration, etc.) on the membrane efficiency, *id est* the log reduction value (LRV), was analyzed as well as effect of operating conditions such as filtration duration. The results obtained are reported and discussed in the present paper.

2. Material and methods

2.1. Membranes

Regenerated cellulose ultrafiltration membranes purchased from Millipore were used for this study. Membrane samples consist in disks of 13.4 cm^2 of effective area with a nominal molecular weight cut-off of 30 kDa. They present an asymmetric structure: skin with low porosity and macroporous support. The thickness of the whole membrane was evaluated to 185 ± 20 µm by dial indicator (Lyssy) whereas the one of the skin to 50 µm by optical profiler (Veeco).

This type of membranes was chosen because preliminary tests showed that they were initially totally retentive towards the selected bacterial strain (*Escherichia coli*). In such conditions, after deliberately altering the membrane integrity, the measurement of the bacterial concentration in permeate samples allows us to quantify bacterial transfer through the artificial defect.

Before the bacterial challenge tests, each membrane was prepared according to the following procedure:

- Compaction: sterile distilled water was filtered through the membrane at a transmembrane pressure of 1.5 bar until the flux had stabilized, after a filtration period of approximately 1 h.
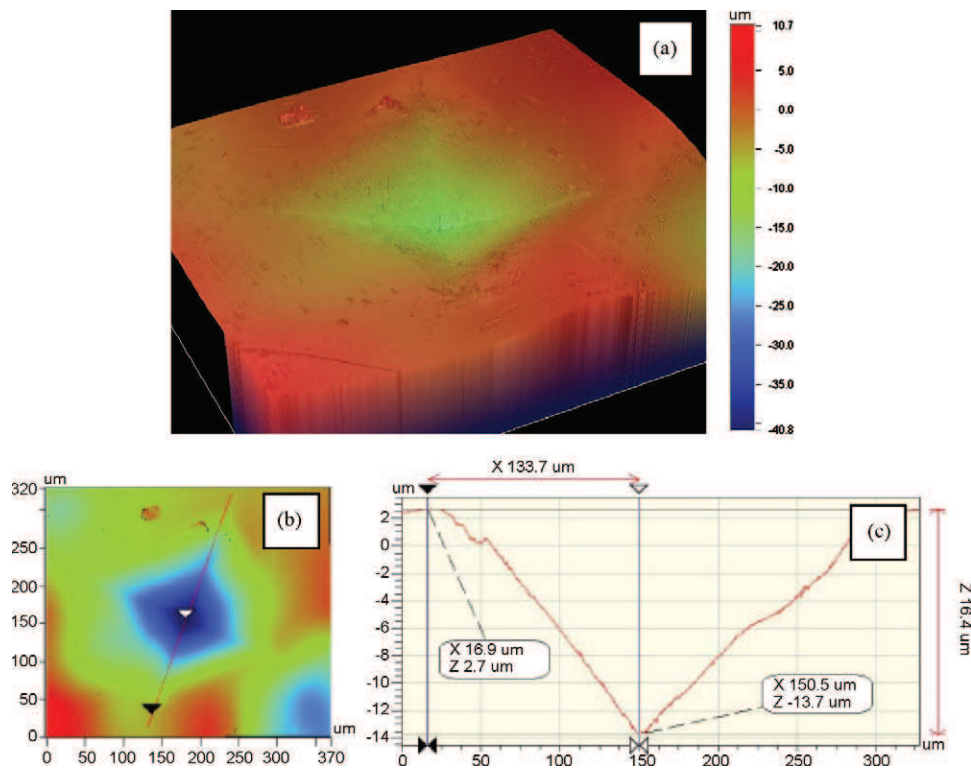
Fig. 1. Optical profiler observations (Veeco) of a defect generated by the microhardness tester with a 50 g load. (a) Oblique plot (colored scale corresponds to depth); (b) surface map; (c) surface profile. (For interpretation of the references to color in this figure legend, the reader is referred to the web version of the article.)

- Measurement of the membrane permeability by water flux tests performed at three different pressures (0.25–0.5–1.0 bar). The permeability of an uncompromised membrane was evaluated to around 220 L/(h m^2 bar) at 20 °C.
- Perforation of the membrane (see Section 2.2).
- Disinfection: the membrane was soaked in a dilute solution of sodium hypochlorite at 200 ppm for 20 min and then rinsed thoroughly with sterile distilled water.
- Measurement of the permeability of the compromised membrane.

2.2. Methods for making defects

The membrane porous structure was altered by perforating the filtering surface by means of various techniques.

First, a microhardness tester (Shimadzu, HMV-2) as those used for characterizing the mechanical properties of materials allowed us to create defects of variable depth. Depending on the load applied by indenter on the membrane, it is possible to punch or not the whole thickness of the membrane skin. For instance, Fig. 1 illustrates the case of a defect altering only part of the skin. The shape of these defects is pyramidal due to the type of indenter used in this study (Vickers). Note that with this technique, no damage could be identified to the membrane support.

Two categories of damages can be made through both skin and macroporous support. On the one hand, mechanical punching through the membrane was performed with a sharp tungsten tip, of the kind used as atomic force microscopy tips. This tip was prepared by electrochemical thinning according to a procedure described by Ibe et al. [17]. Its shape and dimension are depicted in Fig. 2. We made sure that the tip punched through the whole membrane cross-section. The defect diameter was about 200 μm and the shape irregular as shown in Fig. 3. Ultrafast pulsed laser technology allows to burn holes of regular shape. This technique leads to very little heat diffusion hence with no damage apart

from the targeted area. A straight, right cylindrical capillary was made through the skin and support. The diameter of such capillaries was varied between 5 μm (Lightmotif – The Netherlands) and 200 μm (Impulsion – France). The number of holes punched through each membrane sample depends on their diameter. We calculated the approximately number of defects of each size in order to maintain a bacterial concentration in the permeate beyond the detection limit with the lowest possible uncertainty on the log reduction value. A picture in Fig. 4 shows examples of such defects.

2.3. Bacterial suspensions and concentration evaluation during filtration

The bacterial strain selected for this study is *E. coli* (CIP 54127). This strain was chosen for its non-pathogenic bacterium of well defined dimensions (2 μm × 1 μm [18]). In addition, this strain fulfils several important experimental criteria: no need of either
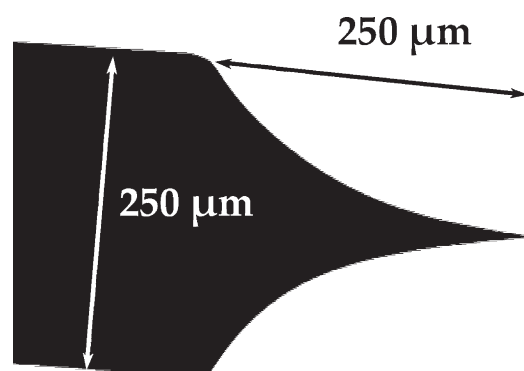

Fig. 2. Optical microscopic observation (Zeiss, Oxilab) of the tungsten tip prepared by electrochemical thinning.
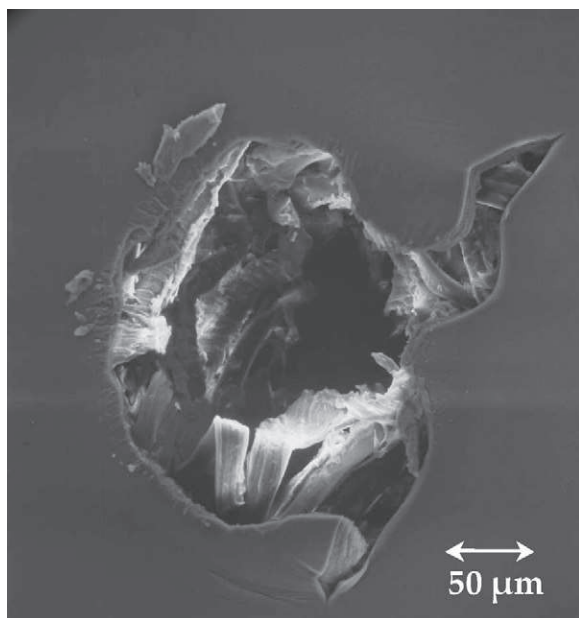
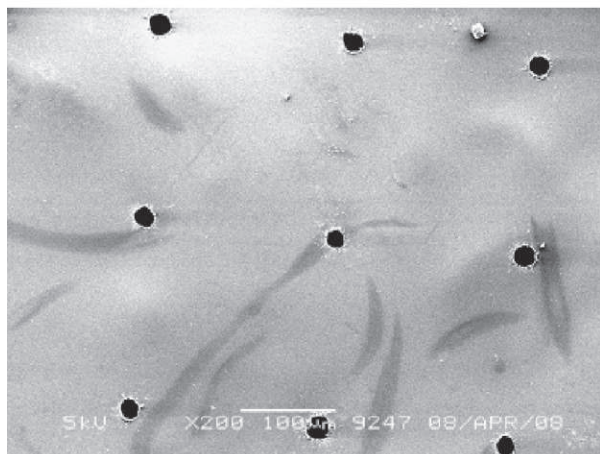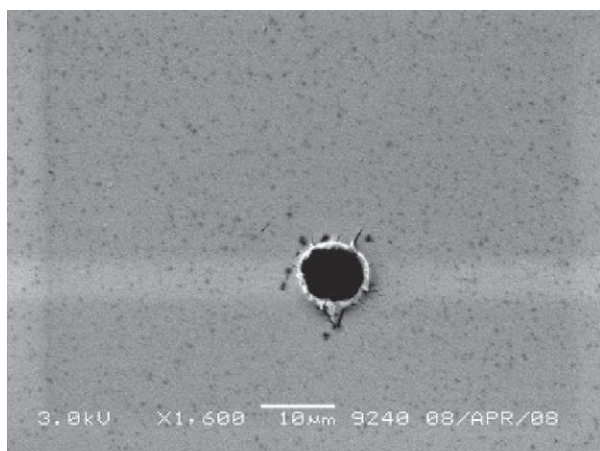**Fig. 3.** Scanning electron microscope image (Hitachi, S-450) of a defect generated by the tungsten tip.

Fig. 4. Scanning electron microscope images (Jeol, JSM 5600 LV) of defect(s) generated by laser impulses.
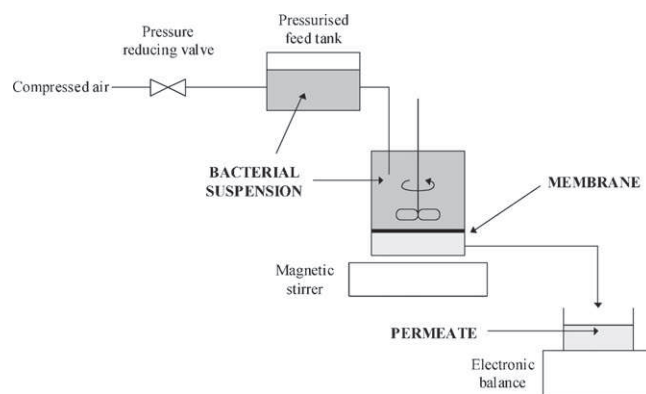

Fig. 5. Experimental set-up.

specific media or specific atmosphere to be grown, short generation time which allows results after overnight incubation.

The bacterial suspension used for the challenge tests was prepared in NaCl aqueous solution at 9 g/L (corresponding to an ionic strength of 150 mmol/L at a concentration of 10^4 cells/mL according to a procedure detailed elsewhere [11]. We choose this concentration since beyond it, the measured retention appeared to increase with concentration (data not shown here), and below this value, the sensitivity of the measure was too low for the purpose of a membrane characterization. The use of an isotonic solution for bacterial suspensions avoids osmotic shock which allows maintaining bacteria size equilibrium and viability over the filtration test duration. This latter criterion was controlled by evaluating the concentration of the feed suspension at the beginning and at the end of the run.

Bacterial concentrations in permeate, retentate and feed solutions were determined by enumeration of the colony forming units (CFU) after tenfold dilutions series, inclusion in tryptone soy agar medium and overnight incubation at 37 °C (see [11] for details). The membrane retention efficiency is evaluated using the log reduction value (LRV) according to the following relationship:

$$LRV = \log \frac{C_r}{C_p} \tag{1}$$

where C_r and C_p are the bacterial retentate and permeate concentration (CFU/mL), respectively.

Our protocol includes whenever necessary, the concentration of the permeate by filtration through nitrocellulose filters (Millipore). The filter was then placed on a tryptone soy agar plate and incubated at 37 °C for 24 h. The enumeration of CFU on the filter allows the determination of very small permeate concentrations. In these conditions, the highest value of the LRV that could be claimed in our experiments was 7.

In addition, we evaluated the number of cells collected on the membrane surface during the filtration run. For this purpose, the membrane was slightly shaked with sterile glass beads of 4 mm in diameter in a non-ionic surfactant (Tween 80 at 10%, Sigma–Aldrich). The bacterial concentration of the resulting suspension was determined by enumeration after tenfold dilution series and inclusion in tryptone soy agar medium.

2.4. Bacterial challenge test and experimental set-up

Bacterial challenge tests were performed using the set-up sketched in Fig. 5. It consists in a dead-end filtration stirred cell of 50 mL content (Model 8050, Amicon) fed from a pressurized tank with the bacterial suspension (see Section 2.3).

This experimental set-up was chosen for its small size which allows an easy disinfection and manipulations under laminar air

flow. Prior to the experiment, the filtration cell was soaked in a concentrated solution of sodium hypochlorite (1000 ppm) for 30 min and all other pieces of equipment were sterilized (20 min at 120 °C).

Each experiment was performed at room temperature and the stirring rate was kept constant over all the experiments at 300 rpm. As the shear stress is non-uniform over the membrane in such stirred cells, the results, and especially the retention ones, should not be directly compared to those obtained with a different set-up geometry (e.g. plate and frame or hollow fiber).

The pressure on the permeate side was atmospheric under all conditions and the transmembrane pressure was adjusted in the range: 0.25–1.00 bar by a pressure reducing valve located on the feed side.

The permeation flux (m s^{-1}) was measured with an accuracy of $\pm 10^{-6}$ m s^{-1} by timed collection of permeate using an electronic balance (Ohaus) assuming a density of 1 kg/L for water. For each run, bacterial feed suspension and retentate were sampled at the beginning and at the end of the experiment for subsequent analysis. Permeate samples were also collected periodically during the experiment in order to monitor the evolution of bacterial concentration.

Each experiment was performed twice. If during these two runs, differences in LRV obtained in the same conditions were larger than ± 0.25, the experiment was triplicate.

3. Theoretical approach

3.1. Mass balance equations and calculated log reduction value

The experimental results obtained using the ultrafast pulsed laser technology described in the previous section had to be analyzed according to a mass balance performed on the microorganisms quantity between the feed and the permeate side of the membrane. In our calculations, we assumed that the corrupted membrane was in fact the combination of one integer membrane of permeability Lp which fully rejects *E. coli* and a few capillary defects, through which the flux of permeate J_d had to be calculated. Moreover, we have considered that bacteria could flow through such capillary with a convective hindrance factor K_c that can be calculated using the Deen correlations [19] (see annex). The smaller dimension of the bacteria (1 μm) has been used in K_c calculation. For defect diameter D_d of 5–200 μm, the convective hindrance factor K_c ranges from 1.3235 to 1.0099.

These calculations assume that long range interactions between the bacteria and pore wall are absent (neutral particle on centerline position in pore). In our system zeta potential of the bacteria has been measured at −16.2 mV and regenerated acetate membrane exhibits a zeta potential around −2 mV [20]. As a consequence, repulsive electrostatic interactions occur. According Deen [19] if interactions are repulsive, there will be a bias toward particle positions near the centerline, and the centerline hydrodynamic approximation will be even more accurate than for neutral particle. Only for attractive interactions is there likely to be a problem.

Thus, in the case of a membrane presenting N_d defects of the same diameter D_d, we obtained the following mass balance equation:

$$C_f K_c J_d N_d D_d^2 = C_p \left(J_d N_d D_d^2 + \frac{4}{\pi} \Delta P \frac{Lp}{\mu} A \right) \tag{2}$$

where C_f and C_p are the bacterial feed and permeate concentration, respectively, A is the effective membrane area, ΔP is the transmembrane pressure and μ the fluid viscosity. We use the viscosity of water for the calculation of the mass flow through the pores, assuming that the additional mass transfer resistance corresponding to one bacterium flowing through a pore is accounted for by the hindrance factor K_c.
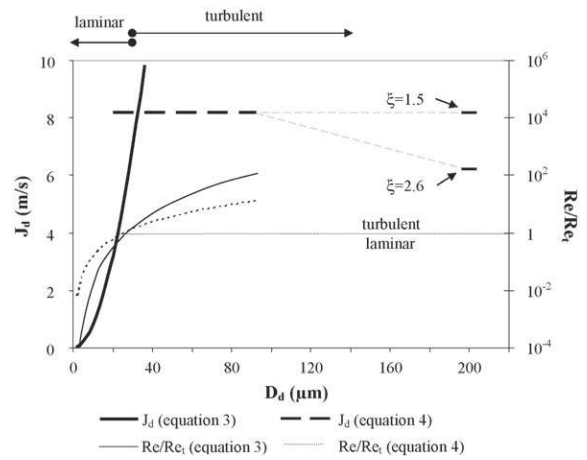

Fig. 6. Evolution of the flow and the associate Reynolds number for a capillary defect of a diameter in the range of 5–200 μm under a transmembrane pressure of 0.5 bar. For the values of diameter ranging from 100 to 370 μm, the evolution of ξ parameter being unavailable, we have reported the results obtained with Eq. (4) by using the two extreme values for ξ: 1.5 and 2.6.

According to van Rijn [21], the equation to be used to calculate the flow through a capillary of diameter D_d under a pressure difference ΔP depends on flow regime and on the ratio of L_d the capillary length (corresponding here to the membrane thickness) to the diameter. The flow regime may be characterized by the comparison of the Reynolds number in the capillary to a transition Reynolds number the value of which is related to the geometrical parameters of the capillary (ratio of the length to the diameter). Thus, for our geometrical conditions (defect diameter of 5–200 μm and membrane thickness of 185 μm), two different equations are needed to describe J_d the flux of permeate through the defect, among which Eq. (3) corresponds to the one proposed by Dagan for laminar flow:

$$\text{for } Re \ll Re_t (\text{laminar flow}), \ J_d = \frac{D_d}{6\pi\mu} \Delta P \left(1 + \frac{16 L_d}{3\pi D_d} \right)^{-1} \tag{3}$$

$$\text{for } Re \gg Re_t (\text{turbulent flow}), \ J_d = \sqrt{\frac{2\Delta P}{\xi\rho}} \tag{4}$$

where μ and ρ are the viscosity and the density of the fluid, respectively.

ξ is an empirical kinetic contribution constant, the value of which depends on L_d/D_d [21]:

for $2 < (L_d/D_d) < 50$ corresponding in this work to $3.7 < D_d < 92.5$ μm; then $1 < \xi < 1.5$,
for $L_d/D_d < 0.5$ corresponding in our study to $D_d > 370$ μm; then $\xi = 2.6$.

Fig. 6 shows the evolution of the flow and the corresponding Reynolds number obtained with the two former equations for a capillary defect of a diameter in the range of 5–100 μm under a transmembrane pressure of 0.5 bar and by using $\xi = 1.5$ in the turbulent flow region. Thus, for the small defects ($D_d < 26$ μm), we will use Eq. (3) to evaluate the flow through the defect whereas Eq. (4) will be used for the larger defects ($26 < D_d < 100$ μm).

For the values of diameter ranging from 100 to 370 μm, the flow regime is still turbulent (Eq. (4)) but the ratio of the length to the diameter of the defect corresponds to an intermediate case between 0.5 and 2 (0.925 for the defect 200 μm in diameter in our experimental part). The evolution of ξ parameter being unavailable in this case, we have then reported in Fig. 6 the results obtained with Eq. (4) by using the two extreme values for ξ: 1.5 and 2.6. In the fol-

lowing the choice will be done to keep the value of ξ constant and equal to 1.5.

Once J_d has been evaluated with Eq. (3) or (4), LRV_0 the initial log reduction value for the separation can be calculated using the following equation:

$$LRV_0 = \log \frac{C_f}{C_p} = \log \left(\frac{1}{K_c} \left(1 + \frac{4\,\Delta P L p A}{\pi N_d D_d^2 J_d \mu} \right) \right) \qquad (5)$$

Through the examination of this equation, it appears that the log reduction value is depending not only on the number of defects per membrane area but also on the effective membrane area. Thereby, Eq. (5) can be expressed in its general form as follows:

$$LRV_0 = \log \frac{C_f}{C_p} = \log \left(\frac{1}{K_c} \left(1 + \frac{4\,\Delta P L p}{\pi n_d D_d^2 J_d \mu} \right) \right) \qquad (6)$$

where n_d is the number of defects per area unit.

In the considered range of conditions, the response of the model is almost independent of the thickness of the membrane (i.e. the length of the defect) whereas very dependent on the diameter of the hole.

Other parameters of the system (permeability and trans-membrane pressure) have a moderate influence. An increased permeability or a larger total membrane area causes an increase in the solvent flux across the integer fraction of the membrane. This increase leads to a dilution of the permeate that increases the calculated removal value, although the bacteria transfer through the defect remains unchanged.

On the other hand, an increase in transmembrane pressure simultaneously induces an increase in the flow of solvent through the integer part of the membrane and an increase in convective flux through the defect (that leads to an increase in transferred microorganisms). Given that the calculated LRV increases with the pressure, the effect of dilution of the permeate seems, at least for the studied geometry, dominant as compared to the increase in convective transfer of *E. coli* through the defect.

Considering our assumptions that the pore flow is not altered by the bacterial concentration, the mass balance from which the LRV calculation is derived is independent of concentration.

In the rest of this paper, Eq. (6) is used to compare the calculated initial log reduction value to the experimental one.

Moreover, this equation may also be used to evaluate the membrane tolerance for defects, namely to determine the set (n_d, D_d) which corresponds to a given initial log reduction value.

3.2. Log reduction value deduced from flux measurements

On the same mass balance principle, by comparing the membrane permeability measured without and with the defect(s), one can calculate a log reduction value deduced from experimental flux measurements:

$$LRV = \log \left(\frac{Lp_d}{Lp_d - Lp} \right) \qquad (7)$$

where Lp and Lp_d are the permeability of the integer and of the compromised membrane, respectively.

3.3. Log reduction value deduced from bacterial concentration: correction for the number of defect per unit area

In order to be able to compare experimental results obtained with various numbers of defects, we need to correct them for the number of defects per unit area. For this purpose, we assume that all defects are working exactly in the same way, which leads to the following equation:

$$LRV_1 = LRV_{N_d} + \log N_d + \log \left(\frac{Lp}{Lp_d} \right) \qquad (8)$$

where LRV_1 and LRV_{N_d} are the log reduction values obtained for one or N_d defects per membrane sample, respectively.

4. Results

4.1. Influence of the defect characteristics

In order to evaluate effects of membrane skin or macroporous support alterations on bacterial retention, the first step of our study was to assess the influence of the defect characteristics upon the log reduction value (LRV). For this purpose, a set of four experiments were performed at constant transmembrane pressure (0.5 bar) and with an *E. coli* feed concentration of around 10^4 CFU/mL. Each membrane has one single defect obtained with one of the techniques presented in Section 2.2 as sketched in Fig. 7. As uncompromised membranes are fully rejective towards *E. coli*, the bacterial concentration in the permeate depends on the transport of the microorganisms through the defect.

The LRV data of the bacterial challenge tests are reported versus the volume of filtrate (Fig. 8). The general observation is that the LRV increases over time (or filtered volume) when flux decreases (results not reported). Permeate flux decrease suggests that membrane is gradually fouled by either the bacteria or extracellular substances (exopolysaccharides) produced by *E. coli* that are recognized for their high fouling index [22,23]. Different tools have been used in order to evaluate the validity of this assumption. An analysis of fouling mechanisms with a method based upon the study of the membrane hydraulic resistance evolution leads to the identification of a "cake filtration" mechanism. On the other hand, the amount of bacteria brought to the membrane surface during the filtration run was evaluated to less than one layer; one cannot speak of cake formation in this case. We then assume that, in our experimental conditions, polysaccharides significantly contribute to the membrane fouling mechanism. Finally, scanning electronic images of the membrane surface after the filtration run show a clogging of the defect carried out with the sharp tip in tungsten whereas it is not the case for the defect carried out with the laser beam (Fig. 9).
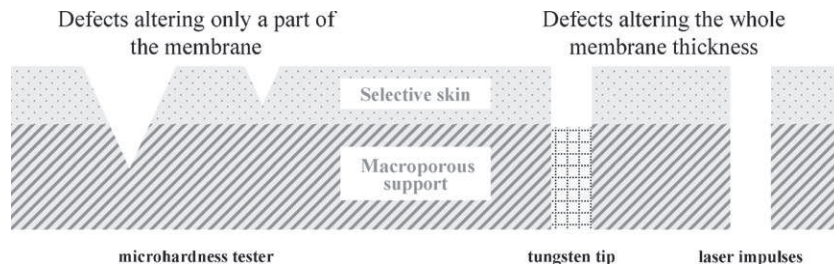

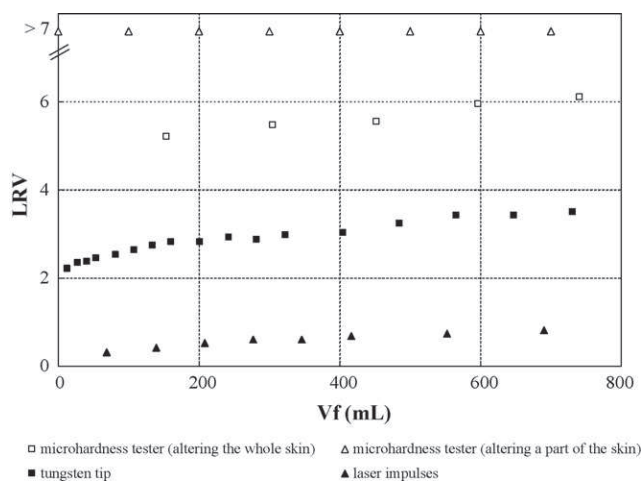**Fig. 7.** Diagrammatic representation of the defects' geometrical characteristics.

Fig. 8. Evolution of the log reduction value (*LRV*) versus the cumulated filtered volume (*Vf*) during filtration at 0.5 bar of *E. coli* on membranes altered with one single defect of various geometrical characteristics.

All these results seem to show that the LRV evolution is resulting from the combination of several phenomena the relative importance of which is not determined at this point of the study. As a consequence, whatever was the origin of this evolution, in order to overcome the previously described phenomena and to allow the comparison of the different challenge tests, in the following part of the study, we use the LRV extrapolated at *Vf* = 0.

First, the comparison between the results obtained for the membranes perforated with the microhardness tester allows to distinguish the role of the membrane skin and macroporous support towards bacterial retention. One expects that the selective skin provides the leading part of the bacterial removal, which is confirmed by the results as in the case of a defect altering only part of the skin, no bacteria was detected in the permeate (LRV > 7). Thus, as long as the skin is not altered on its whole thickness, the membrane keeps a retention efficiency equivalent to the one of an uncompromised membrane. In addition, since the skin is scratched on its whole thickness, bacteria are likely to be transported through the permeate side of the membrane. For the membrane the skin of which was fully punched by the microhardness tester without damage to the macroporous support, the bacterial transfer through the defect is highly limited. Fig. 8 shows that over the time of our experiments and for the membrane used, the membrane support itself was efficient at keeping the LRV higher than 4, despite one pinhole in a 13.4 cm² disk.

Then, by comparing the results of the two other filtration runs, namely those obtained on membrane perforated either with the tungsten tip or with the laser, we get a better understanding of the retention mechanisms provided by the macroporous support. Both defects are altering the whole thickness of the membrane and present a diameter of *ca* 200 μm. The results show that the average retention is higher when the membrane was punched by the tip (around 2.2 log at the beginning of the run versus only 0.3 log for membrane perforated by laser impulses) and the increase in LRV during the experiment is also higher in this case. These results are consistent with the membrane permeability data, which increase from 6.11×10^{-13} m (220 L/(h m² bar)) at 20 °C (uncompromised membrane) to respectively 7.22×10^{-13} m (260 L/(h m² bar)) and 6.67×10^{-13} m (240 L/(h m² bar)) for the membrane presenting a 200 μm defect performed either with the laser beam or the tungsten tip. SEM images taken after both experiments allow to explain the observed discrepancy in terms of water flux and bacterial removal. In Fig. 9, one can see a very large difference in the aspect of

the defects. For the tungsten defect, it seems that the support network, which has been damaged by the tip, has been squeezed by the membrane pressurization, therefore forming a sort of network of polymer filaments, on which adherent bacteria can be seen in the picture. In the case of the laser-made defect, this change in material structure is not possible as the polymer fibers was not pushed away but fully burnt by the femtosecond laser beam. Under such conditions, we conclude that the macroporous support works as quite an efficient fibrous particles collector (and not as a screen), thus preventing bacteria from leaking in the permeate. However, bacteria could be later released in the permeate. As a consequence, a highly compromised membrane (one defect of 200 μm diameter for an effective area of 13.4 cm², which is equivalent to *ca* 750 defects/m²) is likely to keep non-negligible bacterial removal efficiency thanks
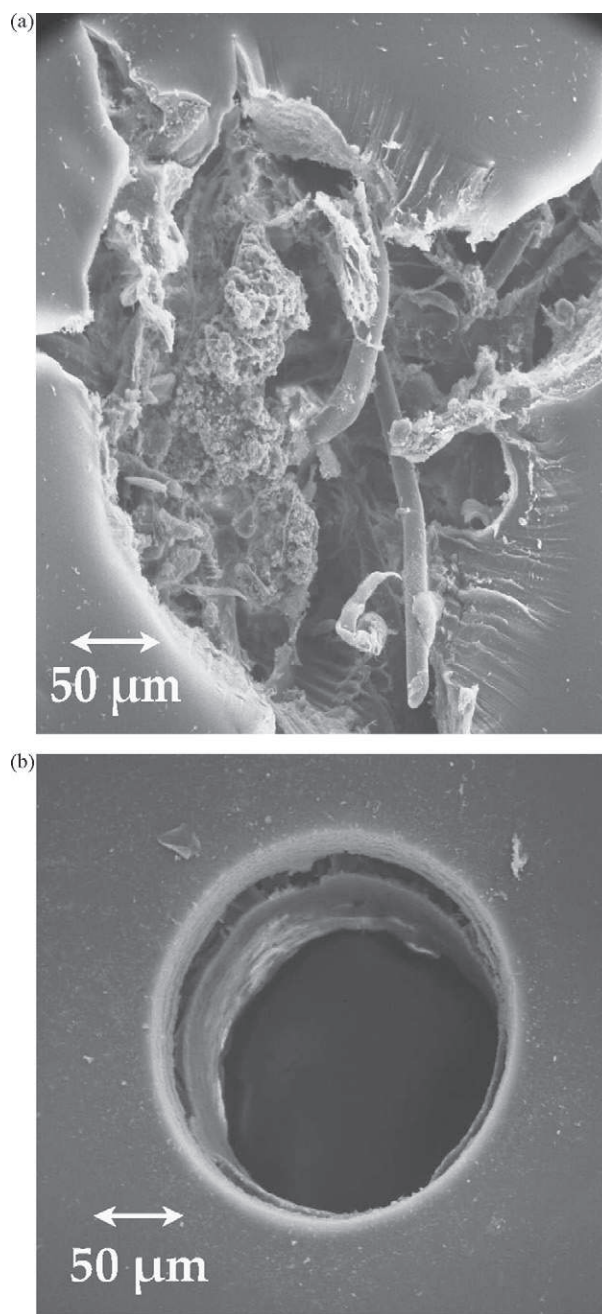

Fig. 9. Scanning electron microscope images (Hitachi, S-450) of defect(s) generated (a) by the tungsten tip and (b) by laser impulses after the filtration of *E. coli* suspension at 0.5 bar.
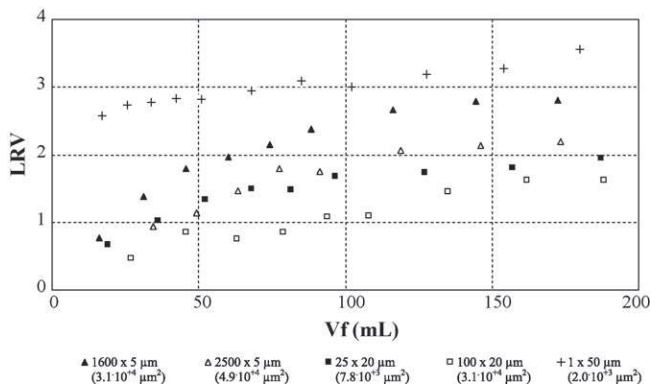
Fig. 10. Evolution of the log reduction value (*LRV*) versus the filtered volume (*Vf*) during filtration at 0.5 bar of *E. coli* on membranes altered with defects generated by laser impulses. Legend mentions number of defects with the given size with in brackets the void area of the membrane sample due to the presence of defects.

to the part taken by the macroporous support in bacteria retention mechanisms.

4.2. Influence of the defect diameter

From Section 4.1, it appears that a defect obtained with a laser beam represents the worst case in terms of bacterial retention. Unlike other kinds of defects, this one is not representative of those which are likely to appear during membrane ageing [13]. However, because of its ideal cylindrical shape, it allows the evaluation of the validity of mass transfer models based on fluid flow through cylindrical channel.

Additional experiments involving membranes with defects generated by laser impulses but of different diameters were performed.

Fig. 10 reports the results obtained with a series of smaller defects. Again the LRV increases along with the cumulated filtered volume and seems to level off beyond around 150 mL. Same reasons as in Section 4.1 could be invoked to explain this evolution. However, unlike the 200 μm diameter defect, a clogging phenomenon of the defect occurs during the filtration run for defects of smaller size as illustrated in the SEM pictures of Fig. 11.
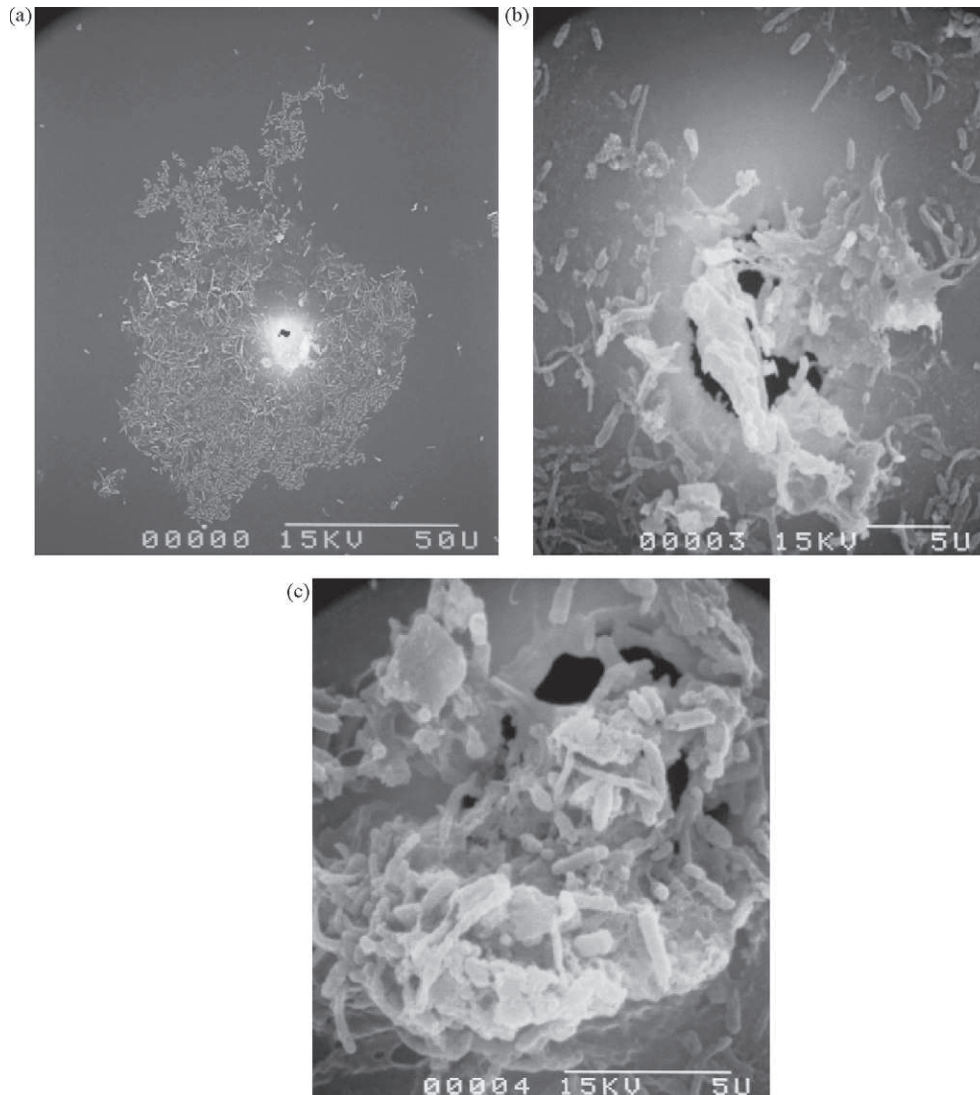

Fig. 11. Scanning electron microscope images (Hitachi, S-450) of defect(s) generated by laser impulses after the filtration of *E. coli* suspension at 0.5 bar. (a) 20 μm diameter, (b) and (c) 5 μm diameter.
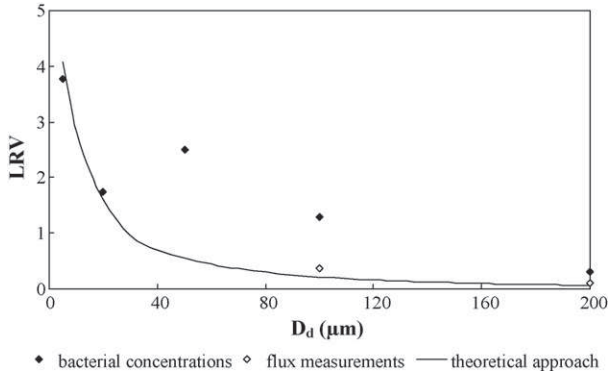
Fig. 12. Log reduction value for one single defect per disk (i.e. 750 defects/m^2) either deduced from bacterial concentrations, from flux measurements or from the short channel flow versus the defect diameter (D_d).

One notices in Fig. 10, that the extrapolated LRV decreases with the number and diameter of defects. In order to compare the initial membrane response obtained with different numbers of defects, we use Eq. (8) introduced in Section 3.3 considering extrapolated log reduction value for LRV_{N_d}. Using Eq. (7) (Section 3.2), we evaluate a LRV from permeability measurements. Results are reported in Fig. 12 which shows the LRV for one single defect per disk (i.e. 750 defects/m^2) either deduced from flux measurements or from concentration measurements in permeate and retentate. Concerning the LRV deduced from flux measurements, we consider only the data for the defects of 100 and 200 μm as for the smaller diameters the change in permeability was within the experimental error. We confirm that the water permeability is insufficient to detect the presence of a 50 μm diameter defect in a 13.4 cm^2 ultrafiltration membrane [16].

For the two larger diameters, LRV obtained from flux measurements or bacterial concentrations do not give same results, which suggests that the bacterial transport through the defect is hindered as compared to the solvent one. Taking into account the bacterial biological characteristics such as their motility is not sufficient to explain these results [24–26].

Using the pore flow model (Eq. (3) or (4) and Eq. (6)) to calculate LRV (see Section 3.1), a good agreement is observed between calculated and experimental data.

Our experiment, that we duplicated, shows a singularity for defects at 50 μm that we could not explain within the duration of the project. To explain and understand this phenomenon, subsequent experiments should be implemented with larger membrane area and a greater number of defects per unit area. However, the model is consistent for defects of 5 and 20 μm in diameter, joins the asymptote for 200 μm defects and the calculated LRV values remain always lower than the experimental ones. This provides a model to estimate the effect of a given number of defects of the same diameter on the bacterial retention capacity of a filter, in worse conditions, *id est* before membrane fouling has started changing the membrane properties. Thus, despite the proposed model is not fully predictive, it allows evaluating the minimum number of defects of a given diameter that characterization methods have to be able to detect in order to ensure a water of a given microbiological quality.

5. Conclusion

This experimental study of ultrafiltration of *E. coli* suspension shows that although the integer skin of an asymmetric ultrafiltration membrane offers the best protection against bacterial contamination of the permeate, a scratched UF membrane surface still retains microorganisms to a significant level. We observed, under our conditions that a 200 μm pinhole punched with a sharp object in a 13.4 cm^2 lowers the LRV from 7 to *ca* 2, whereas the LRV decreases down to almost zero if a cylindrical pore of the same diameter is preformatted through the membrane. This observation underlines the clear difference between those two types of defects: conclusions obtained with membranes corrupted with type of defects should therefore not be extended to membranes showing the other type.

As expected, membrane fouling enhanced the bacterial retention at least over the 4 h duration of our experiments.

Assuming that the viscosity in the pores is equal to the water viscosity, and that bacteria adsorption on the pore walls plays a negligible role in bacteria retention a model based on a "short channel assumption was used. We show that it underestimates the retention of *E. coli* for capillaries in the range of *ca* 50–200 μm in diameter. This suggests that the flow of bacteria was slowed down by some additional phenomenon that we could not identify. The transmission of bacteria in pores of smaller (5–20 μm) pores is, on the other hand, better predicted by such convective flows.

Appendix A.

Calculation of convective hindrance factor K_c using the Deen correlations [19]:

$$K_C = \frac{(2 - \phi)\, K_s}{2K_t}$$

$$\phi = \left(1 - \frac{D}{D_d}\right)^2$$

$$\binom{K_t}{K_s} = \frac{9}{4}\pi^2\sqrt{2}\left(1 - \frac{D}{D_d}\right)^{-5/2}\left[1 + \sum_{n=1}^{2}\binom{a_n}{b_n}\left(1 - \frac{D}{D_d}\right)^n\right] + \sum_{n=0}^{4}\binom{a_{n+3}}{b_{n+3}}\left(\frac{D}{D_d}\right)^n$$

The coefficient in K_t and K_s are:

$a_1 = -73/60$, $a_2 = 77.293/50.400$, $a_3 = -22.5083$, $a_4 = -5.6117$, $a_5 = -0.3363$, $a_6 = -1.216$, $a_7 = 1.647$;
$b_1 = 7/60$, $b_2 = -2.227/50.400$, $b_3 = 4.0180$, $b_4 = -3.9788$, $b_5 = -1.9215$, $b_6 = 4.392$, $b_7 = 5.006$.

In these equations D is the bacteria diameter and D_d the defect diameter.

Nomenclature

A	membrane area (m^2)
C_f	bacterial feed concentration (CFU/mL)
C_p	bacterial permeate concentration (CFU/mL)
C_r	bacterial retentate concentration (CFU/mL),
D	bacteria diameter (m)
D_d	defect diameter (m)
J_d	flux of permeate through the defects (m s^{-1})
K_c	convective hindrance factor from Deen correlations
L_d	capillary length, corresponding to the membrane thickness (m)
L_p	permeability of the uncompromised membrane (m)
Lp_d	permeability of compromised membrane (m)
n_d	number of defects per surface unit (m^{-2})
N_d	number of defects
ΔP	transmembrane pressure (Pa)
Re	Reynolds number in the defect
Re_t	transition Reynolds number
Vf	filtered volume (m^3 or mL)

Greek letters

μ	viscosity of the fluid (Pa s)
ρ	density of the fluid (kg m^{-3})
ξ	empirical kinetic contribution constant

References

[1] V. Lazarova, P. Savoye, M.L. Janex, E.R. Blatchey, M. Pommepuy, Advanced wastewater disinfection technologies: state of the art and perspectives, Water Sci. Technol. 40 (4–5) (1999) 203–213.

[2] K. Farahbakhsh, Monitoring the integrity of low-pressure membranes, J. Am. Water Works Assoc. 95 (6) (2003) 95–107.

[3] N. Adams, P. Côté, An evaluation of membrane integrity monitoring methods for micro- and ultrafiltration systems, in: 10th Aachen Membrane Colloquim Proceeding, 2005.

[4] S. Giglia, M. Krishnan, High sensitivity binary gas integrity test for membrane filters, J. Membr. Sci. 323 (2008) 60–66.

[5] P. Aimar, M. Meireles, V. Sanchez, A contribution to the translation of retention curves into pore size distributions for sieving membranes, J. Membr. Sci. 54 (1990) 321–338.

[6] T. Urase, K. Yamamoto, S. Ohgaki, Effect of pore size distribution of ultrafiltration membranes on virus rejection in crossflow conditions, Water Sci. Technol. 30 (9) (1994) 199–208.

[7] T. Kobayashi, M. Ono, M. Shibata, N. Fujii, Cut-off performance of *Escherichia coli* by charged and noncharged polyacrylonitrile ultrafiltration membranes, J. Membr. Sci. 140 (1998) 1–11.

[8] M.H. Shinde, S.S. Kulkarni, D.A. Musale, S.G. Joshi, Improvement of the water purification capability of poly(acrylonitrile) ultrafiltration membranes, J. Membr. Sci. 162 (1999) 9–22.

[9] T. Suchecka, E. Biernacka, W. Piatkiewicz, Microorganism retention on micro-filtration membranes, Filtr. Sep. 40 (2003) 51–55.

[10] T. Suchecka, W. Piatkiewicz, T.R. Sosnowski, Is the cell retention by mf membrane absolutely safe—a hypothetical model for cell deformation in a membrane pore, J. Membr. Sci. 250 (2005) 135–140.

[11] N. Lebleu, C. Roques, P. Aimar, C. Causserand, Role of the cell-wall structure in the retention of bacteria by microfiltration membranes, J. Membr. Sci. 326 (2009) 178–185.

[12] S. Rouaix, C. Causserand, P. Aimar, Experimental study of the effects of hypochlorite on polysulfone membrane properties, J. Membr. Sci. 277 (2006) 137–147.

[13] A.J. Gijbertsen-Abrahamse, E.R. Cornelissen, J.A.M.H. Hofman, Fiber failure frequency and causes of hollow fiber integrity loss, Desalination 194 (2006) 251–258.

[14] V. Gitis, R.C. Haught, R.M. Clark, J. Gun, O. Lev, Application of nanoscale probes for the evaluation of the integrity of ultrafiltration membranes, J. Membr. Sci. 276 (2006) 185–192.

[15] V. Gitis, R.C. Haught, R.M. Clark, J. Gun, O. Lev, Nanoscale probes for the evaluation of the integrity of ultrafiltration membranes, J. Membr. Sci. 276 (2006) 199–207.

[16] C. Causserand, P. Aimar, C. Vilani, T. Zambelli, Study of the effects of defects in ultrafiltration membranes on the water flux and the molecular weight cut-off, Desalination 149 (2002) 485–491.

[17] J.P. Ibe, P.P. Bey, R.A. Brandow, R.A. Brizzolara, N.A. Burnham, D.P. Dilella, K.P. Lee, C.R.K. Marrian, R.J. Colton, On the electrochemical etching of tips for scanning tunneling microscopy, J. Vac. Sci. Technol. A 8 (4) (1990) 3570–3575.

[18] S.A. Biondi, J.A. Quinn, H. Goldfine, Random motility of swimming bacteria in restricted geometries, AIChE J. 44 (8) (1998) 1923–1929.

[19] W.M. Deen, Hindered transport of large molecules in liquid-filled pores, AIChE J. 33 (1987) 1409–1425.

[20] M.M. Rohani, A.L. Zydney, Effect of surface charge distribution on protein transport through semipermeable ultrafiltration membranes, J. Membr. Sci. 337 (2009) 324–331.

[21] C.J.M. van Rijn, Nano and micro engineered membrane technology, Membrane Science and Technology Series, 10, Elsevier B.V. Ed., Amsterdam (2004).

[22] S. Nataraj, R. Schomacker, M. Kraume, I.M. Mishra, A. Drews, Analyses of polysaccharide fouling mechanisms during crossflow membrane filtration, J. Membr. Sci. 308 (2008) 152–161.

[23] G. Zhang, S. Ji, X. Gao, Z. Liu, Adsorptive fouling of extracellular polymeric substances with polymeric ultrafiltration membranes, J. Membr. Sci. 309 (2008) 28–35.

[24] H.C. Berg, L. Turner, Chemotaxis of bacteria in glass capillary arrays, Biophys. J. 58 (1990) 919–930.

[25] Z. Liu, W. Chen, K.D. Papadopoulos, Bacterial motility, collisions and aggregation in a 3-μm-diameter capillary, Biotechnol. Bioeng. 53 (1997) 238–241.

[26] K.C. Chen, R.M. Ford, P.T. Cummings, Mathematical models for motile bacterial transport in cylindrical tubes, J. Theoret. Biol. 195 (1998) 481–504.